



Feasibility study on multi-seam upward mining of multi-layer soft–hard alternate complex roof

Yuben Liu^{1,2} · Jiulong Cheng^{1,2} · Junjun Jiao^{1,2} · Xiangxi Meng³

Received: 9 November 2021 / Accepted: 21 July 2022 / Published online: 23 August 2022
© The Author(s), under exclusive licence to Springer-Verlag GmbH Germany, part of Springer Nature 2022

Abstract

Multi-seam upward mining is of considerable importance to improve the resource recovery rate and realize waste-free mining. Taking the Dianping coal mine in Shanxi Province as an example, the development height and evolution process of the overburden fracture after mining of the Taiyuan Group coal seam were studied by combining theoretical analysis, field measurement, and numerical simulation to verify the feasibility of upward mining (UM) of the multi-layer soft–hard alternate complex roof of Taiyuan group coal seam in Shanxi Province, China. A new method for determining the development height of overburden fractures (DHOF) is proposed on the basis of analyzing the fracture characteristics of rock strata with different lithologies. This method first calculates the fracture of key strata and then that of key soft rock strata controlled by key strata. The above method found that the DHOF of the Dianping coal mine is 52.5 m, and the field measurement and numerical simulation results are 53 and 49.7 m, respectively. The numerical simulation study found that after the upper and lower coal seams were mined, the rock fissures between the two seams were only connected to a small extent near the open-off cut, and most of the area still impermeable. Therefore, using the proposed method in UM is feasible after simple reinforcement of the rock seam in the vicinity of the open-off cut. In addition, on-site field measurements applied the borehole resistivity method to present a dynamic all-round view of the overburden fracture development process, and monitoring results indicate the existence of an unconnected fracture zone at the top of the fracture zones. Research results provide an important theoretical and technical basis for the prediction of the development height of the overlying rock fracture zone and the feasibility of UM in the Taiyuan coalfield, Shanxi Province.

Keywords Upward mining · Development height of overburden fractures · Key soft rock strata · Multi-layer soft–hard alternate complex roof · Borehole resistivity method

Introduction

As China's most important energy, coal production and consumption are expected to still account for more than half of China's total energy by the year 2030 (Hu et al. 2020a;

Zhu et al. 2020). In recent years, many mines in western China have opted for upward mining. The main reason is to increase the output of the mine and improve the recovery rate of resources to achieve non-waste mining (Bai et al. 2018). UM refers to mining the lower coal seam first and then the upper coal seam in the process of multi-coal seam mining. The overlying strata of the lower coal seam are broken and bent after their mining, and the caved zones, fractured zones, and continuously deformed zones are formed from bottom to top of the goaf (Fig. 1), in which the fracture zone is the key range affecting the UM (Cheng et al. 2017; Huang et al. 2018; Sun et al. 2019, 2020; Zhang et al. 2018). Different from conventional mining, UM focuses on the stress and deformation law of strata between upper and lower coal seams, especially the control layer, to describe the essential process of strata movement in UM accurately (Zhong 2011). In addition, accurately determining the maximum height

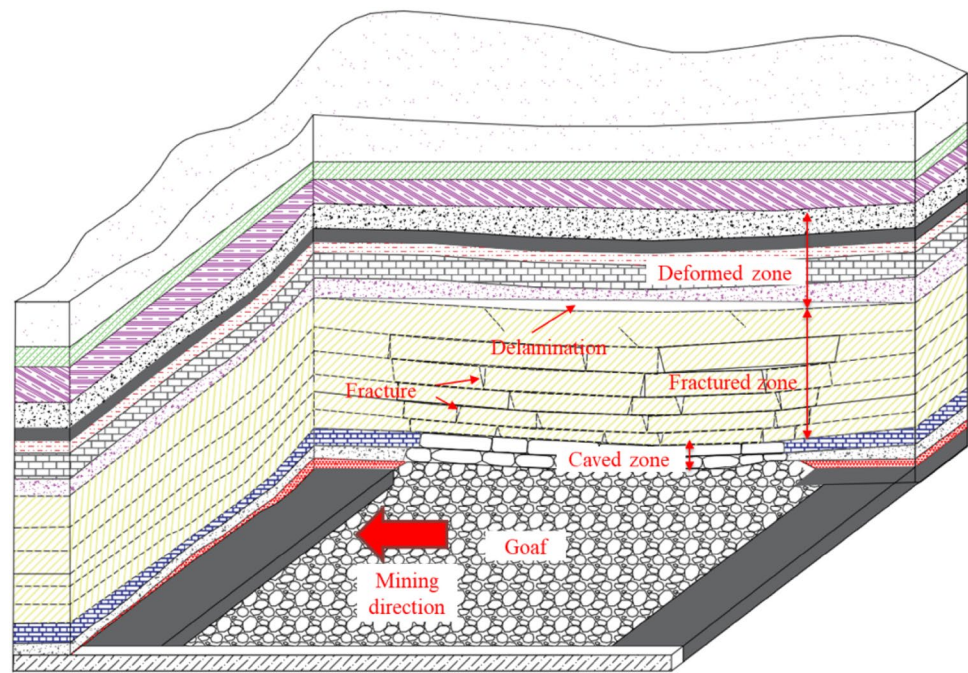
✉ Jiulong Cheng
jlcheng@cumtb.edu.cn

¹ State Key Laboratory of coal resources and safe mining, China University of Mining and Technology (Beijing), Beijing 100083, China

² College of Earth Science and Surveying Engineering, China University of Mining and Technology (Beijing), Beijing 100083, China

³ College Of Safety And Environmental Engineering, Shandong University of Science and Technology, Qingdao 266590, China

Fig. 1 Three zones above the goaf



of the overburden fracture after lower coal seam mining is crucial for UM to avoid the floor heave problem during upper coal seam mining (Wu et al. 2017a). Therefore, the aforementioned condition is the key to realizing UM and improving resource recovery rates to grasp the fracture evolution law of upper and lower coal seams after mining and determine the maximum height of the overburden fracture zone in lower coal seam mining accurately.

The current research shows that the rock below the key strata is broken when UM is conducted, the loose and broken rock mass has improved the supporting effect, and the development of fractures is restrained. However, the roof rock in the lower seam of conventional mining is prone to several activations under repeated mining action, and the fracture development is complete (Cui et al. 2019a). In addition, the microseismic signal monitoring shows that the cumulative energy in the UM process is less than that of traditional mining (Cui et al. 2019b). Therefore, the UM of multiple coal seams is conducive to the stability of overlying strata. Moreover, the key to determining the feasibility of UM is to identify the height of the overlying rock fracture zone after mining in the lower coal seam. The methods for predicting the height of the overlying rock fracture include empirical formula, theoretical analysis, physical test, field measurement, and numerical simulation (Ren and Wang 2020; Wei et al. 2017; Hou et al. 2020; Hu et al. 2020b; Liu et al. 2015). For instance, Majdi proposed five mathematical methods to estimate the development height of overburden fractures (DHOF) based on the analysis of geological structures (Majdi et al. 2012). Moreover, Wang further found that the height of overburden fracture development is related to

the distance between the main key strata and mined coal seam based on key strata theory (Wang et al. 2019). Many machine learning algorithms have been applied to predict the DHOF with the rapid development of artificial intelligence technology (Wu et al. 2017b; Li et al. 2015). An increasing number of studies on the rules of overburden fracture development in the geological conditions of western China have been conducted in recent years due to the rising proportion of coal production in western China in the national energy supply. Among these studies, Zhu investigated the calculation method of the overburden fracture zone height in bedrock and loess strata in northwestern China based on plate–shell theory (Zhu et al. 2020). Liu used borehole water monitoring technology and distributed optical fiber sensing technology to measure the height of water-conducting fissures in the overburden of soil–rock composite structures in western China (Liu et al. 2019).

The above studies provide good insights into the prediction of DHOF under general geological and demonstrate the feasibility of UM. However, the following deficiencies are observed. (1) The feasibility of UM is examined on the basis of the DHOF after lower coal seam mining, and the connectivity of the fractures after mining upper and lower coal seams is then verified. (2) The strata with similar lithology are artificially assumed to be the same type of strata during the height prediction of overburden fracture development. However, the overlying strata of Taiyuan Formation in Shanxi Province, China, are characterized by complex lithology, multiple layers, and thin thickness of single-layer strata, alternate soft–hard strata, and large differences in physical and mechanical parameters of strata

with similar lithology. Therefore, a large error is found in the calculation of strata with similar lithology assumed to be the same strata. (3) Field measurement technologies include borehole camera observations, double-end plugging leakage, packer tests, and slug tests (Cheng et al. 2020; Liang et al. 2020; Adhikary and Guo 2015; Karacan and Goodman 2009). These methods only obtain the DHOF statically and do not show the entire process of overburden fracture initiation–expansion–development–stability dynamically. Therefore, field measurement should be further improved.

This paper aims to analyze the feasibility of UM of the multi-layered soft–hard alternate complex roof. A new method suitable for calculating the overburden fracture development height of coal seam in the Taiyuan Formation is proposed on the basis of the fracture characteristic analysis of rock strata with different lithologies. Moreover, the borehole resistivity method is used to monitor the overlying rock fractures in the mining process of working face dynamically, which not only obtains the development height of overlying rock fractures but also acquires their development and change processes. Finally, the numerical simulation is used to verify the connectivity of the fractures after mining the upper and lower coal seams, and the feasibility of UM of the Taiyuan Formation coal seam is comprehensively determined.

Engineering geological information

General information of the Dianping coal mine

Dianping coal mine, which belongs to HuoZhou Coal Electricity Group Co. Ltd., located in Dianping village, Fangshan County, Lvliang City, Shanxi Province, China, is shown in Fig. 2. The minefield area is 13.53 km², geological reserves are 140 million tons, recoverable reserves are 80 million tons, and mine design production capacity is 260 t/year. The coal-bearing strata in the minefield are mainly Taiyuan Formation of Carboniferous. The development mode of this mine is inclined shaft development, and the comprehensive mechanized mining method with a long wall is adopted. The current main mining coal seam is 9#, and the un-mining coal seam is 5#.

Engineering geologic information

The No. 9-204 working face is located in the left part of the second mining area of 830 m level. The east side of the working face is the boundary of the minefield, the west side is the 830 system roadway, the south side is the unexploited coal seam, and the north side is adjacent to the No. 9-202 working face. The No. 9-204 working face during mining remains unaffected by surface water, in which the direct water filling source is roof limestone aquifer water mainly

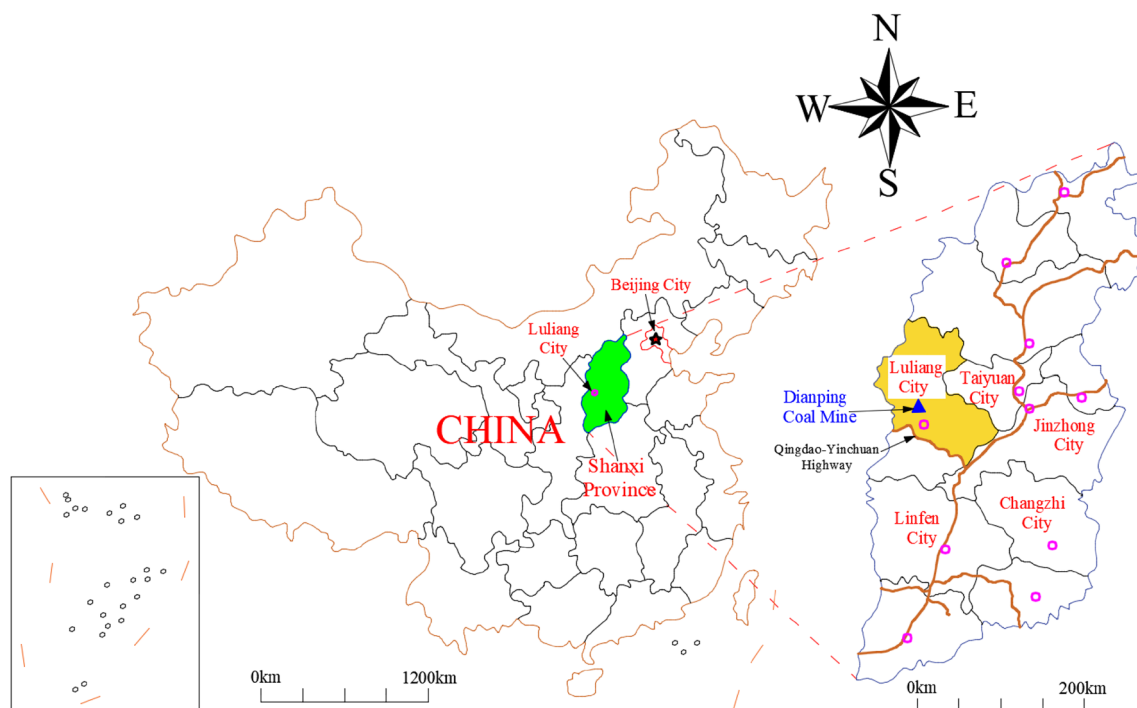


Fig. 2 Location of the Dianping coal mine

through the rock fissure into the working face. The recoverable coal seam overlying the working surface of No. 9-204 is No. 5 coal seam, and the distance between Nos. 5 and 9 coal seams is 64–69 m. No. 5 coal seam remains un-mined during the mining of No. 9 coal seam. The layout of the working face is shown in Fig. 3.

Hydrogeological information

The hydrogeological data of Dianping Mine show that there are five aquifer strata in the mine, among which the karst fracture aquifer of Carboniferous Taiyuan Formation is within the stratigraphic range of this study. The karst fracture aquifer of Carboniferous Taiyuan Formation is mainly composed of three layers of limestone with thickness of 2.4, 6.5 and 8.4 m, respectively. Limestone fractures developed and the core is broken. During the exploration in 2005, when the three layers of limestone were drilled, all of them showed an increase in water consumption. According to the pumping test data, the unit water inflow of the aquifer is 0.009–0.078 L/s-m, the permeability coefficient is 0.054–0.2713 m/d, and the water level elevation is +935.04 to +1058.70 m. Overall, the water-rich aquifer is weak, the water quality is $\text{HCO}_3\text{-SO}_4\text{-Na}$ type, and the salinity is 0.4642 g/L.

Methodology

Theoretical analysis

The overlying strata of coal seam have different lithologies, strengths, and thicknesses. These overlying strata of coal seam can be roughly divided into hard and soft rocks according to their strength. Several rock mechanics tests show that hard and soft rocks are, respectively, prone to brittle and plastic failure (Zhao et al. 2019b; Zhang et al. 2017; Wu

and Gao 2010; Yang et al. 2018). Therefore, a large error is observed in the previous method of calculating the height of overburden fracture development, which regards the entire rock group as a unified whole and ignores the lithological characters of rock strata. The fracture of hard and soft rocks is calculated in this paper through various ways to obtain an accurate height of overburden fracture development. The feasibility of UM is finally determined by comparing the maximum height of overburden fracture development with the distance between Nos.9 and 5 coal seams.

Mechanical analysis of overlying key strata fracture

Engineering practice shows that rock movement is usually not a separate process. However, through a layer of high strength, thick hard rock is a key stratum that supports the upper multiple soft rock synchronous coordinated movements (Qian et al. 2010). The calculation prerequisite for the height of the overburden fracture development is to determine the position of key strata in overburden accurately. Rock strata are determined as key strata according to the key strata theory to meet the following:

$$\begin{cases} q_1(x)_{m+1} < q_1(x)_m \quad (m = 1, 2 \dots n) \\ l_k + 2H_k \cot \alpha < l_{k+1} + 2H_{k+1} \cot \alpha \quad (k = 1, 2 \dots n) \end{cases} \quad (1)$$

where $q_1(x)_m$ is the load of the m th layer rock strata on the first strata, N ; l_k is the breaking distance of the k th hard strata, m ; and n is the number of hard strata; H_k is the vertical distance between the hard rock strata of the k th layer and the mining coal seam; α is the breaking angle of hard strata.

The entire rock stratum produces rotary deformation with the hinge of the section contact point when the key strata are incompletely broken (Zhou 2017). The stress geometric model of rock strata is shown in Fig. 4a.

The geometric relationship in the figure and plastic hinge theory reveal the following:

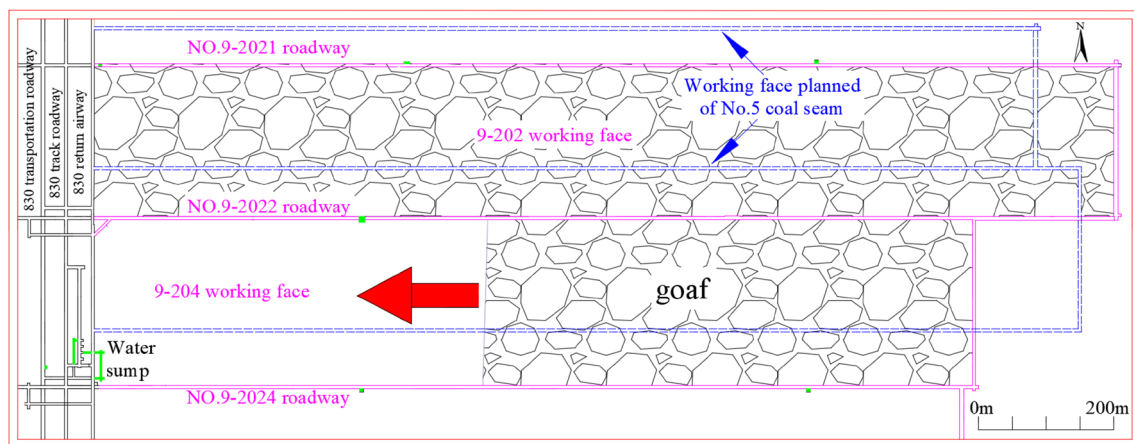
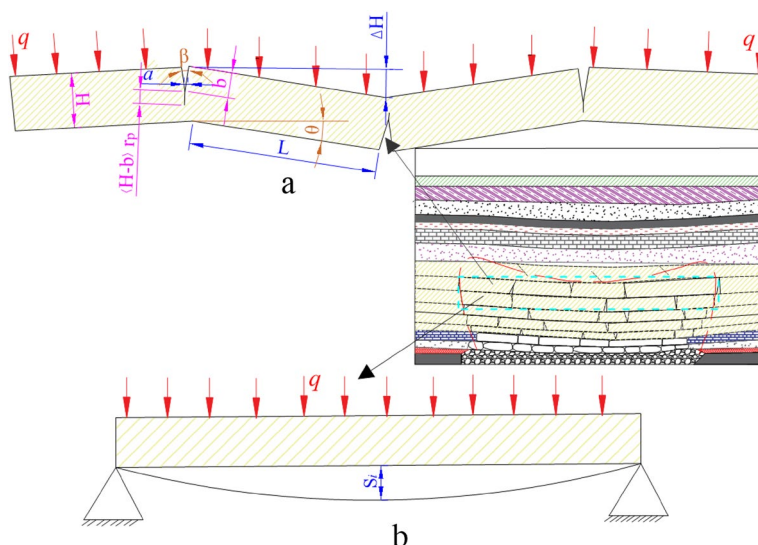


Fig. 3 Working face layout of No. 5 and No. 9 coal seam

Fig. 4 The rock strata stress geometric model



$$\Delta H = M - h_z(K_z - 1) - (h_i - h_z)(K_i - 1) = L \sin \theta \quad (2)$$

$$\beta = \frac{a}{(H - b)r_p} \quad (3)$$

where ΔH is the subsidence value of rock strata, m; M is the mining thickness of coal seam, m; h_z is the thickness of the immediate roof, m; h_i is the vertical distance between the i th layer rock strata and the coal seam roof, m; K_i is the rock fragmentation coefficient of the i th layer above the immediate roof; K_z is the rock fragmentation coefficient of the immediate roof; L is the length of the broken rock ($L = \frac{1}{2}l_k$), m; θ is the rotation angle of rock fracture; a is the length of the fracture tip opening; b is the length of longitudinal fracture; H is rock thickness, m; r_p is the rotation factor of the plastic hinge; and β is the fracture opening angle.

The rock beam bending moment formula and the test proved that the fracture opening angle is smaller than that of the rock fracture rotation angle at the beginning of the fracture stage (Zhang 2016). However, the continuous expansion of the rock fracture resulted in two approximately equal angles, that is, $\theta = \beta$. Substituting Eq. (3) into Eq. (2) yields the following:

$$\Delta H = \frac{1}{2}l_k \sin \frac{a}{(H - b)r_p} \quad (4)$$

$$b = H - \frac{a}{r_p \arcsin(2\Delta H/l_k)} \quad (5)$$

The concept of connectivity introduced in the literature indicates that connectivity refers to the proportion of rock fractures in the thickness direction of rock strata (Huang et al. 2010). Combined with the geometric relationship in Fig. 4a, connectivity is presented as follows:

$$D = b/H = 1 - \frac{a}{r_p H \arcsin(2\Delta H/l_k)} \quad (6)$$

The relationship between the periodic fracture interval and the connectivity in the literature revealed that the rock stratum has undergone complete fracture when the connectivity exceeds 0.9 (Huang et al. 2010). The adjacent vertical fissure will be connected due to the transverse crevasse propagation of rock strata when the connectivity exceeds 0.5, thus eventually forming the connected fissures. Meanwhile, fissures in the rock stratum will not form connected fissures when the connectivity is less than 0.5, and the development of the fracture zone is terminated. It is worth noting that this criterion is applicable to hard rock strata in this study.

Fracture mechanics analysis of KSRS controlled by key strata

The definition of key soft rock stratum (KSRS) is the soft rock stratum with the strongest deformation resistance in the soft rock group controlled by key strata. Soft rock has a strong deformation resistance, and its fracture mode is different from hard rocks. The study shows that the fracture of soft rock strata can be determined by their horizontal tensile amount. Therefore, the soft rock strata in overburden can be simplified as a fixed beam model (Fig. 4b).

The deflection curve function and boundary conditions of the fixed beam model can be, respectively, given as follows (Zhao et al. 2019a; Guo and Lou 2018):

$$\omega = \sum_{n=1}^{\infty} A_n \left(1 + \cos \frac{2(2n - 1)\pi x}{l} \right) \quad (7)$$

$$\begin{cases} \omega|_{x=0}=0, \frac{d\omega}{dx}|_{x=0}=0 \\ \omega|_{x=l}=0, \frac{d\omega}{dx}|_{x=l}=0 \end{cases} \quad (8)$$

where l is the length of the fixed beam, which is numerically equal to the rock-breaking interval. Furthermore, the condition for balancing Eq. (7) is as follows:

$$EI \frac{d^4\omega}{dx^4} - q(x) = 0 \quad (9)$$

where inertia moment I can be expressed as $I = bh^3/12$, $b = 1$; E is the elastic modulus of soft rock strata; q is a load of soft rock strata; and h is the thickness of soft rock strata.

A deflection curve function after deformation can be obtained by substituting Eqs. (7) and (8) into Eq. (9).

$$\sum_{n=1}^{\infty} EIA_n \left(\frac{2(2n-1)\pi}{l} \right)^4 \cos \frac{2(2n-1)\pi x}{l} - q = 0 \quad (10)$$

The equation of A_n is obtained using the Galerkin integral formula to calculate Eq. (10):

$$A_n = \frac{ql^4}{8((2n-1)\pi)^4 EI} = \frac{3ql^4}{2\pi^4(2n-1)^4 Eh^3} \quad (11)$$

Therefore, the deflection curve function can be given as shown below by substituting Eq. (11) into Eq. (7):

$$\omega = \sum_{n=1}^{\infty} \frac{3ql^4 \left(1 + \cos \frac{2(2n-1)\pi x}{l} \right)}{2\pi^4(2n-1)^4 Eh^3} \quad (12)$$

The maximum deflection of the clamped beam can be obtained by the following calculation:

$$\omega_{\max} = \frac{5ql^4}{32Eh^3} \quad (13)$$

Horizontal tensile deformation due to bending of clamped beams can be calculated using Eq. (14):

$$\epsilon = \frac{1}{\rho} y \quad (14)$$

where y is the distance from any position on the clamped beam to the neutral layer.

$$\frac{1}{\rho} = \frac{d\theta}{dx} = \frac{d\omega/dx}{dx} = - \sum_{i=1}^n \frac{6ql^2}{(2n-1)^2 E\pi^2 h^3} \cos \frac{2(2n-1)\pi x}{l} \quad (15)$$

By substituting Eq. (15) into Eq. (14), horizontal tensile deformation ϵ can be given as

$$\epsilon = - \sum_{i=1}^n \frac{6ql^2 y}{(2n-1)^2 E\pi^2 h^3} \cos \frac{2(2n-1)\pi x}{l} \quad (16)$$

where n is close to infinity and $y = h/2$, if $\cos \frac{2(2n-1)\pi x}{l} = -1$, then ϵ obtains the maximum value:

$$\epsilon_{\max} = \frac{3ql^2}{8Eh^2} \quad (17)$$

$$l = \sqrt{\frac{8\epsilon_{\max} Eh^2}{3q}} \quad (18)$$

The condition for determining soft rock as KSRS are as follows: If $l_i < l_{i+1}$, then the i th layer of soft rock is the KSRS. In addition, the free space height below soft rock strata can be given as follows:

$$S_i = M - h_z(K_z - 1) - (h_i - h_z)(K_i - 1) \quad (19)$$

The soft rock produces connected fissures when its horizontal tensile deformation value exceeds its critical value, and the maximum deflection is less than its free space height; otherwise, the fractures stop developing.

Calculation method of DHOF

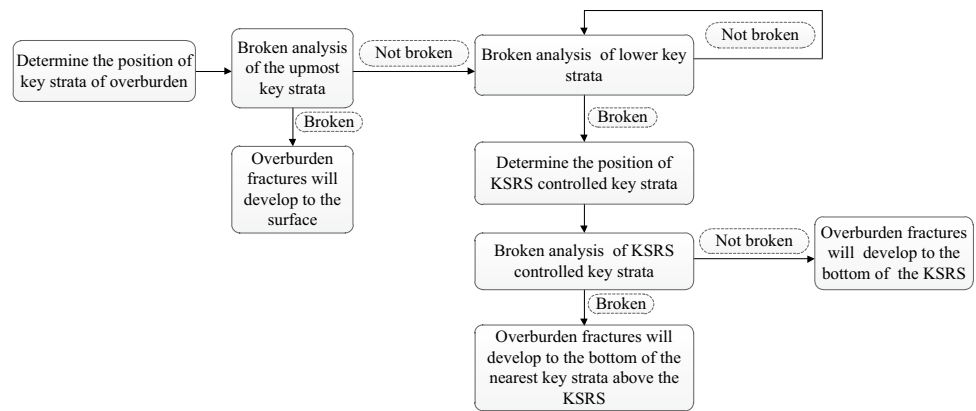
The specific calculation process of DHOF is shown in Fig. 5. First, the fracture of key strata in hard rock is determined. Then, the fracture of KSRS controlled by hard rock is identified. Finally, combined with the overall fracture height of hard and soft rocks, the accurate overburden fracture zone height is obtained.

Field measurements

Dynamic monitoring method and working principle

The borehole resistivity method (BRM) is a full-space electrical exploration method, which is developed on the basis of the conventional high-density resistivity method. This method applies an array of mathematical methods to integrate multiple combinations of electrical sounding and profile systems and uses the detection system for drilling. The basic principle of this monitoring method is still based on the electrical difference between geological anomaly bodies and surrounding rock, and the distribution law of abnormal electric field formed under the action of the artificial electric field is studied. Several electrodes are placed once on each measuring point of the profile according to the designed electrode distance, and a stable current is provided to the surrounding medium through the power supply electrode. The potential difference values at various positions are calculated by the measuring electrode, and the apparent

Fig. 5 Calculation flow chart of overburden fracture development height



resistivity of the recording point is obtained in accordance with the corresponding formula. The distance and position between the power supply and measurement electrodes can be automatically changed regularly by selecting different electrode combinations and spacings through the program control switch. The potential difference values of various positions and depths can be measured, and the data acquisition can be quickly completed.

Monitoring project layout

The dynamic monitoring design of BRM aims to arrange the drilling at 17 m west of the mining stop line of No. 9-2042 roadway in No. 9 coal seam. Drilling was conducted in the drilling chamber, with drilling number 1#, drilling azimuth angle of 56°, elevation angle of 50°, designed drilling length of 94 m, and maximum control height of the detection range of 70 m (above the coal seam roof). The 1# drilling layout is shown in Fig. 6. The BRM uses Wenner device, and electrode is a self-made conductive copper sheet wound on the wire. A total of 44 electrodes are arranged in the 1# drilling, and the electrode spacing is 2 m. The field detection construction equipment and field engineering layout are shown in Fig. 7.

Numerical simulations

Establishment of numerical model

The meshes and domains for numerical calculation with FLAC3D are given in accordance with the strata structure of the roof and floor (Fig. 8) as shown in Fig. 9. The model is discretized into a mesh of X, Y, and Z dimensions of 300 m × 250 m × 145 m, respectively, containing a total of 259,200 zones. The step-by-step excavation method is used to simulate the coal seam mining process. The working face

moves 160 m forward in 16 steps. To eliminate the boundary effect, in the process of model excavation, 50 m coal pillars are set on both sides of the boundary in the y-axis direction and 70 m coal pillars are set on both sides of the boundary in the X-axis direction. All the above calculations are based on the generalized Mohr–Coulomb failure criterion.

Boundary conditions of the numerical model

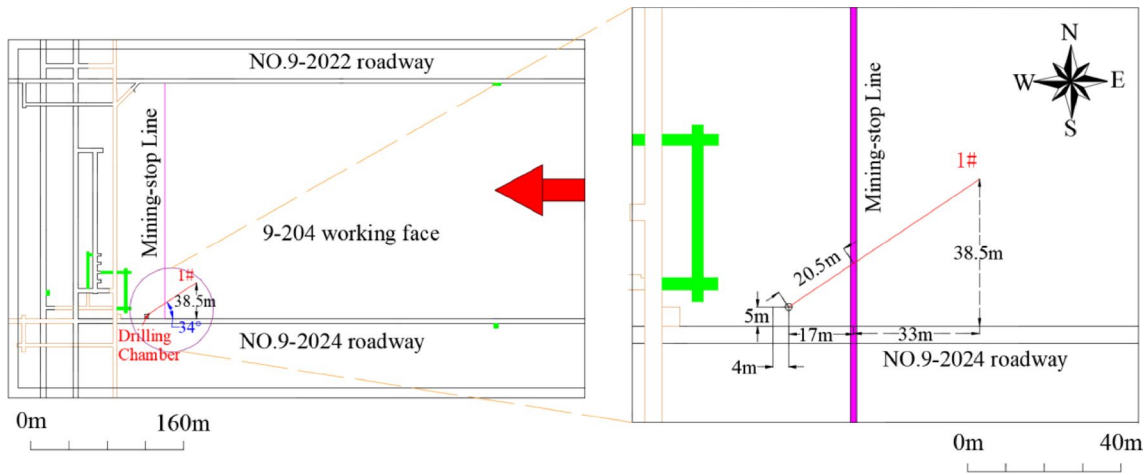
The equivalent uniform load $\sigma_z = 8.5$ MPa is applied on the vertical direction (Z direction) of the model to simulate the in situ stress caused by the overlying strata at a depth of approximately 350 m. In addition, the ratio of vertical stress and horizontal stress (X and Y direction) is 1.2, that is, the horizontal stress is about 7 MPa. Meanwhile, the lower boundary is completely constrained, and the other boundary is horizontally constrained. The model boundary settings are shown in Fig. 10.

The rock mechanics test of the roof and floor strata near the 9-206 working face in the Dianping coal mine (Fig. 11) was conducted, and the accurate physical and mechanical parameters of the strata were obtained. Table 1 outlines the mechanical parameters of different strata used in the numerical model according to the mechanical test data.

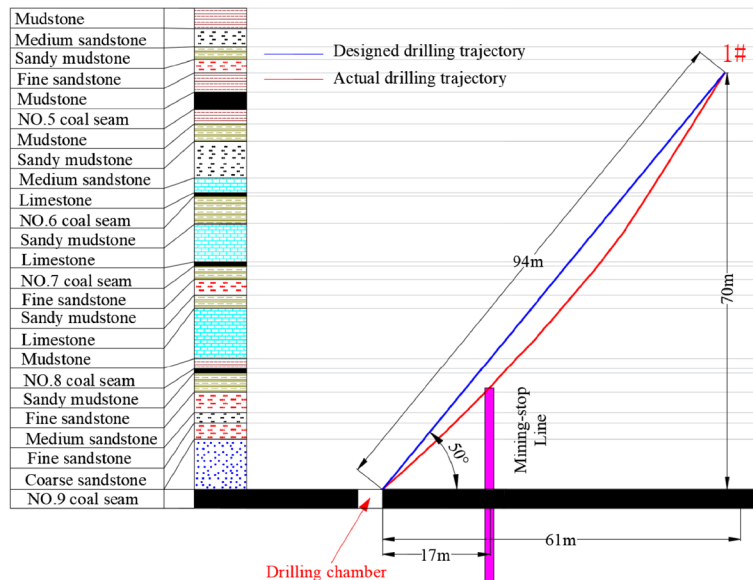
Results and analysis

Theoretical calculation results and analysis

The calculation results of the key strata and the distribution of the soft rock strata are shown in Fig. 8. The rock physical and mechanical parameters of the rock layer are shown in Table 1. The conclusion of the literature research revealed that $r_p = 0.46$ (Zhou 2017), the maximum length of the fracture tip opening in the literature a is 3 mm (Huang



(a) Plane diagram



(b) Section diagram

Fig. 6 Monitoring drilling layout of BRM in No. 9-204 working face

et al. 2010), and the residual expansion coefficient $K_z = 1.15$, $K_i = 1.02$, which are substituted into Eq. (6) to calculate the following: maximum subsiden

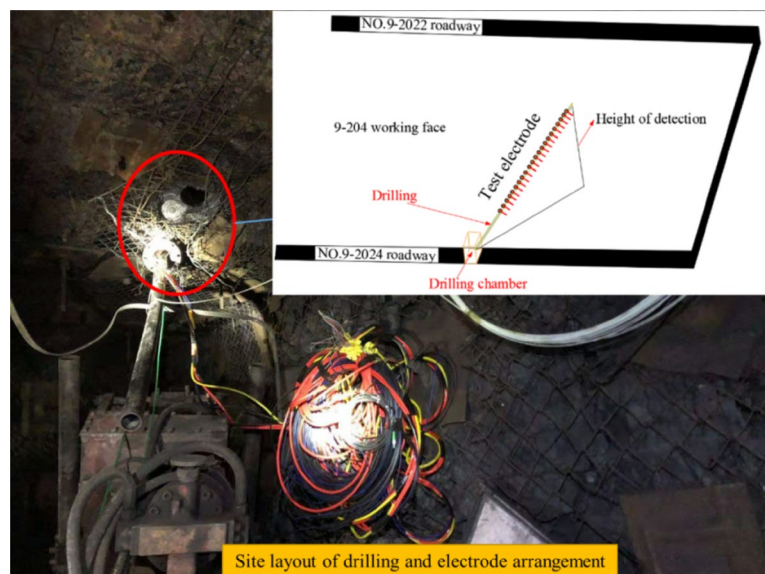
$$D_{ks4} = 1 - \frac{a}{r_p H \arcsin(2\Delta H/l_k)} \tag{20}$$

$$= 1 - \frac{3}{0.46 \times 6.2 \times \arcsin 0.034} = 0.47$$

The calculation results show that the penetration of key strata 4 is 0.47. The parameter is similarly substituted into Eq. (6), and the penetration of key strata 3 is calculated to be 0.73. The criterion in “Theoretical analysis” indicates that key strata 4 will remain unbroken but key strata 3 will break. Therefore, the maximum development range of the fracture zone is between key strata 3 and 4.

Furthermore, the KSRS controlled by key strata 3 is soft rock 5, and its lithology is sandy mudstone. The literature

Fig. 7 The field detection construction equipment and field engineering layout



reveals that the critical horizontal tensile strain of sandy mudstone is 1 mm/m, which is substituted into Eq. (18):

$$l = \sqrt{\frac{8\varepsilon_{\max} E h^2}{3q}} = \sqrt{\frac{8 \times 1 \times 10^{-3} \times 3840 \times 4.6^2}{3 \times 0.063}} = 58.65m \tag{21}$$

The maximum deflection of KSRS can then be given as shown as follows by substituting Eq. (21) into Eq. (13):

$$w_{\max} = \frac{5ql^4}{32Eh^3} = \frac{5 \times 0.063 \times 58.65^4}{32 \times 3840 \times 4.6^3} = 0.52m \tag{22}$$

In addition, the parameters are substituted into Eq. (19) to obtain the maximum subsidence of KSRS:

$$S_i = M - h_z(K_z - 1) - (h_i - h_z)(K_i - 1) = 2.6 - 8.4 \times 0.15 - 36.35 \times 0.02 = 0.613m \tag{23}$$

The determination method in Fig. 5 concluded that the soft rock 5 is broken because $w_{\max} < S_i$, and the fracture develops to the bottom of key strata 4. Combined with the rock depth in Fig. 8, the maximum DHOF can be calculated as 52.5 m.

Field measurement results and analysis

The resistivity curve is shown in Fig. 12, where L is the distance between the mining position of the working face and the stopping line. The apparent resistivity of 12 groups of different detection periods was selected, and the range of overburden fracture development was obtained by analyzing the relationship between drilling depth and resistivity in different mining periods. The change trend of resistivity in Fig. 12a shows that the resistivity of the drilling depth

in the range of 3–59 m remarkably varies during the entire monitoring process, and the change rate of resistivity is larger than 20%. This finding indicates that the rock strata in this range are destroyed under the continuous stress variation, and a large range of continuously connected fractures is formed. On the contrary, the resistivity change rate is less than 5% in the range of 60–79 m drilling depth, and the resistivity is relatively stable throughout the monitoring process, which is an unconnected fracture zone. Figure 12b shows the partial amplification of Fig. 12a. The figure reveals that the resistivity change is the most stable at the position of 77 m in borehole depth. Therefore, the highest position of overburden fracture development affected by mining is at 77 m in borehole depth (the height of overburden fracture development is 53 m). Moreover, the change rate of resistivity in the range of 79–91 m is smaller than that in the range of 3–59 m, and the resistivity is relatively stable during the entire monitoring process. Thus, the range is unaffected by coal mining, but the primary fractures in the strata are relatively developed.

The resistivity detection data before coal seam mining are selected as the background value to display the development process of overburden fractures intuitively and dynamically, and other monitoring data subtract the background value. The inversion processing is then conducted. The difference in apparent resistivity under different monitoring cycles is shown in Fig. 13, where T1 represents the monitoring time.

The resistivity section of overburden failure when the coal face is mined 31 m away from the mining stop line is shown in Fig. 13a. Many continuous high-resistivity areas (area ①) are found in the range of drilling depths of 5–55 m, thus, a large number of unconnected fractures are generated under the influence of mining pressure relief with the mining of No. 9 coal seam. Moreover, two low-resistivity anomaly

Fig. 8 Strata histogram of mining faces

| No. | Thickness (m) | Depth (m) | Lithology | Column | Key strata | Soft rock |
|-----|---------------|-----------|------------------|--------|--------------|-------------|
| 1 | 3.4 | 257.8 | Mudstone | | | |
| 2 | 3 | 260.8 | Medium sandstone | | | |
| 3 | 2.2 | 263.0 | Sandy mudstone | | | |
| 4 | 2.2 | 265.2 | Fine sandstone | | | |
| 5 | 3.3 | 268.5 | Mudstone | | | |
| 6 | 2.9 | 271.4 | NO.5 coal seam | | | |
| 7 | 2.4 | 273.8 | Mudstone | | | |
| 8 | 3 | 276.8 | Sandy mudstone | | | Soft rock 6 |
| 9 | 6.2 | 283.0 | Medium sandstone | | Key strata 4 | |
| 10 | 2.4 | 285.4 | Limestone | | | |
| 11 | 0.6 | 286.0 | NO.6 coal seam | | | |
| 12 | 4.6 | 290.6 | Sandy mudstone | | | Soft rock 5 |
| 13 | 6.5 | 297.1 | Limestone | | Key strata 3 | |
| 14 | 0.7 | 297.8 | NO.7 coal seam | | | |
| 15 | 2.2 | 300.0 | Sandy mudstone | | | Soft rock 4 |
| 16 | 2.7 | 302.7 | Fine sandstone | | | |
| 17 | 2.3 | 305.0 | Sandy mudstone | | | Soft rock 3 |
| 18 | 8.4 | 313.4 | Limestone | | Key strata 2 | |
| 19 | 1.8 | 315.2 | Mudstone | | | Soft rock 2 |
| 20 | 0.7 | 315.9 | NO.8 coal seam | | | |
| 21 | 3.2 | 319.1 | Sandy mudstone | | | Soft rock 1 |
| 22 | 3.5 | 322.6 | Fine sandstone | | | |
| 23 | 1.7 | 324.3 | Medium sandstone | | | |
| 24 | 2.8 | 327.1 | Fine sandstone | | | |
| 25 | 8.4 | 335.5 | Coarse sandstone | | Key strata 1 | |
| 26 | 2.6 | 338.1 | NO.9 coal seam | | | |
| 27 | 2.7 | 340.8 | Fine sandstone | | | |
| 28 | 6.2 | 347.0 | Medium sandstone | | | |

areas are observed in the range of 25–45 m drilling depth (area ②). The elevation position of the low-resistivity anomaly corresponds to the limestone stratum, which contains a small amount of limestone water. Limestone water then enters the fracture zone of the rock stratum along the fracture

diversion channel due to the development and penetration of longitudinal fractures in the rock stratum.

The resistivity section of overburden failure when the coal face is mined 21 m away from the mining stop line is shown in Fig. 13b. The drilling depth range of 5–60 m is a

Fig. 9 The meshes and domains for numerical calculation with FLAC3D

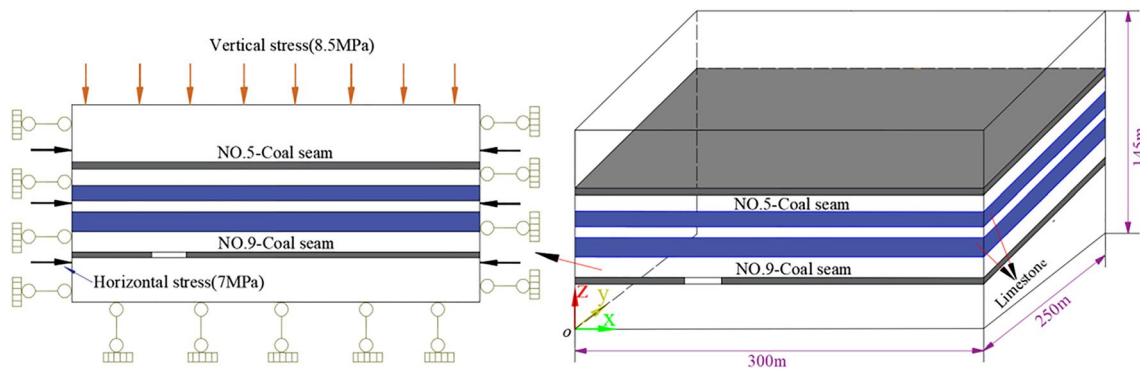
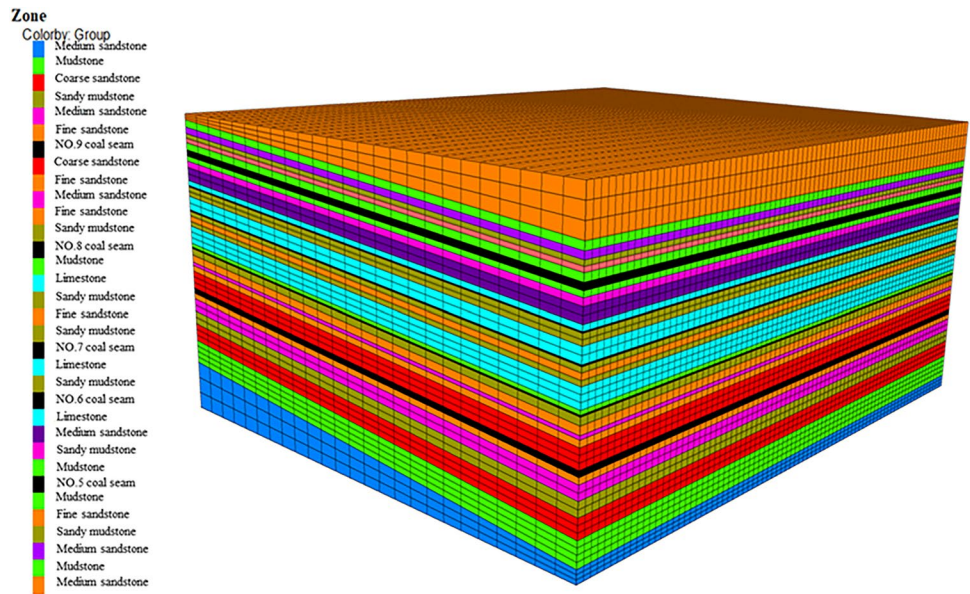


Fig. 10 Boundary condition of numerical model

continuous and relatively regular arc-shaped high-resistance region (area ①), indicating that coal seam mining causes dramatic and evident changes in rock morphology. The longitudinal fractures in the rock expand at this time, and the fractures with different development forms are connected, forming a large area of the overburden fracture zone. The figure reveals that the elevation corresponding to the fracture development height is 886 m (the black dotted line elevation), and the roof elevation of coal seam 9 in this position is 846 m. Therefore, the fracture development height is calculated as $H = 886 - 846 = 40$ m. The fracture development height is determined as the initial fracture development height because it is the first large-scale destruction of rock strata in the process of field dynamic monitoring.

Figure 13c shows the inversion diagram of resistivity change when the working face is 11, 7, 4, and 0 m from the stop line from top to bottom. The change of resistivity in the black wireframe in the figure indicates that the

high-resistivity area in the range of 70–90 m of the drilling depth gradually disappears with the mining of the working face, indicating the compaction of original fractures in this range and the absence of new fractures. The resistivity change in the red-wire frame in the figure can be described as low-high-low. The analysis of the change process is as follows. When the filling medium inside the fracture affected by mining is air, the range of fractures shows high resistivity, while when the filling medium is water, the conductivity of the fracture increases and the range shows low resistivity. Since the limestone strata in the stratum structure of Dianping coal mine are weak aquifers, considering that water is affected by gravity in the changing fractures, it is speculated that the reason of low resistivity in area 2 is that water in limestone infiltrates into mining fractures. Contrary to the area 2, the area 3 shows a relatively high resistance. It is speculated that the reason is that with the mining of the coal seam, a large number of accompanying fractures are

Fig. 11 Test on mechanical parameters of roof and floor strata

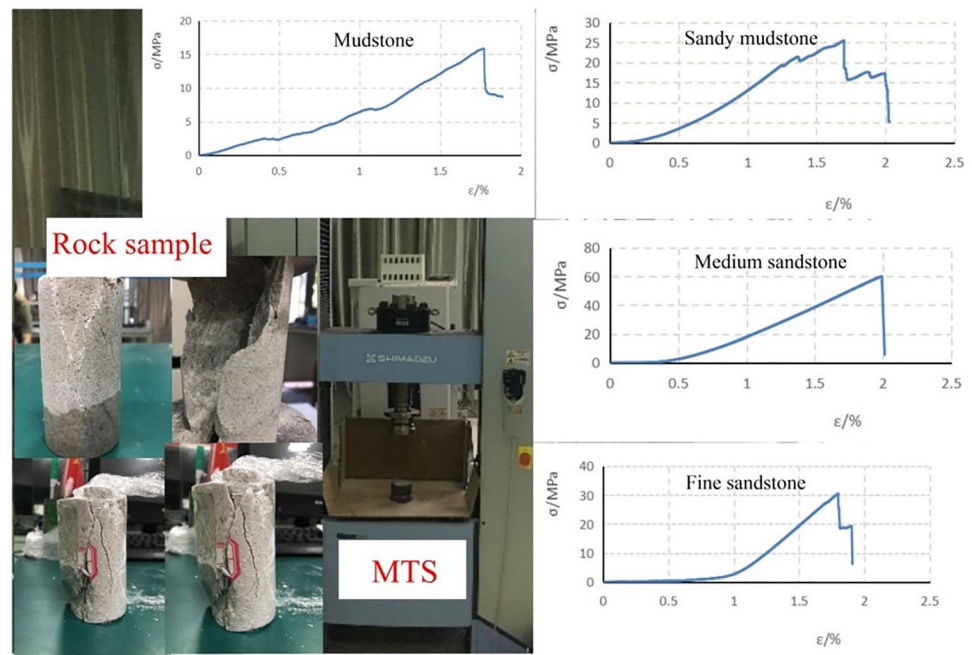


Table 1 The physical and mechanical parameters of different strata

| Layer number | Lithology | Density/(kN m ⁻³) | Elastic modulus/GPa | Bulk modulus/GPa | Shear modulus/GPa | Poisson ratio | Cohesion/MPa | Friction-angle/(°) | Tensile strength/MPa |
|--------------|------------------|-------------------------------|---------------------|------------------|-------------------|---------------|--------------|--------------------|----------------------|
| 1 | Medium sandstone | 25.60 | 3.92 | 2.33 | 1.61 | 0.22 | 5.0 | 34 | 3.50 |
| 2 | Mudstone | 26.99 | 0.81 | 0.64 | 0.31 | 0.29 | 2.8 | 39 | 2.48 |
| 3 | Sandy mudstone | 26.00 | 1.99 | 1.51 | 0.78 | 0.28 | 7.8 | 32 | 3.65 |
| 4 | Fine sandstone | 25.70 | 3.58 | 2.49 | 1.42 | 0.26 | 9.2 | 31 | 8.50 |
| 5 | Coal seam | 14.10 | 1.12 | 0.93 | 0.43 | 0.3 | 0.2 | 20 | 0.20 |
| 6 | Limestone | 28.00 | 8.69 | 4.53 | 3.68 | 0.18 | 11.4 | 38 | 2.70 |
| 7 | Coarse sandstone | 27.00 | 7.92 | 3.77 | 3.44 | 0.15 | 3.0 | 40 | 4.34 |

produced. Due to the connectivity between the fractures, the water in the fractures is lost, and the filling medium in the fractures is changed from water to air, so it is changed from low resistance to high resistance. The resistivity of area 4 is lower than that of area 2. It is speculated that the position may be caused by the retention of limestone water in large fractures.

The resistivity section of overburden failure after stopping mining for 25 days is shown in Fig. 13d. Compared with Fig. 13c, the change in overburden fracture is absent, and only a small range of transverse fractures is found in the range of 70–75 m of drilling depth. Several

discontinuous and unconnected independent fracture areas are observed in the drilling depth of 60–80 m.

The resistivity section of overburden failure after stopping mining for 40 days is shown in Fig. 13e. The overburden movement ends at this time as the stress of the surrounding rock reaches the equilibrium state again, and some fractures are re-compacted. The development height and range of the fracture zone also tend to stabilize. The maximum development height is 77 m in drilling depth, and the corresponding development height of the overburden fracture is 53 m. The minimum distance between Nos. 5 and 9 coal seams is 65 m, which is substantially larger

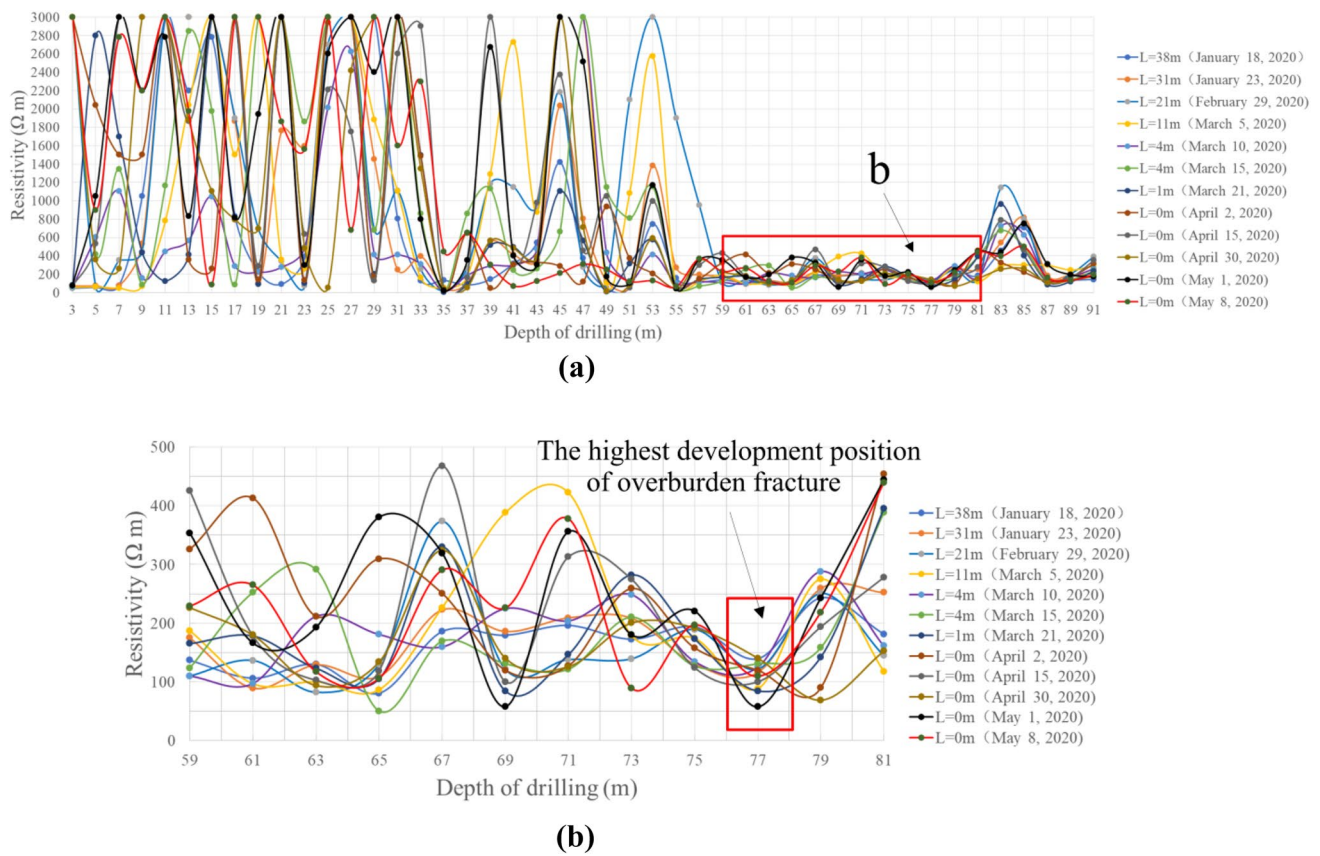


Fig. 12 Resistivity curve of overburden fractures

than the maximum fracture development height monitored in the field.

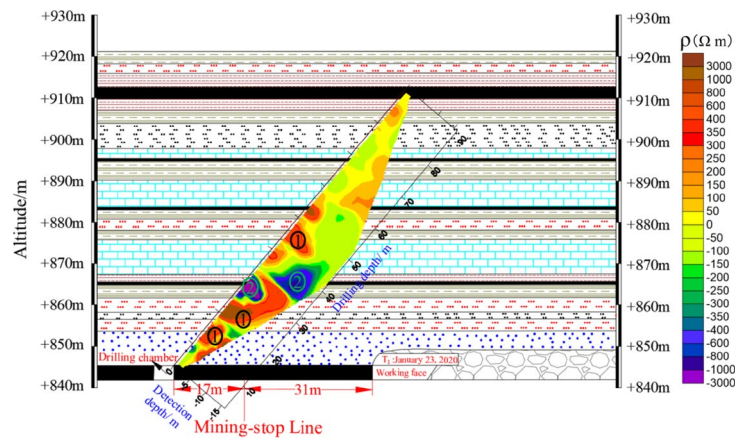
Numerical simulation results and analysis

A simulated 3D perspective view and transverse section of the plastic zone and stress distribution are shown in Fig. 14. After the coal seam is mined, the stresses that were in equilibrium are redistributed, and stress concentrations occur within a range of approximately 5 m in front of the coal mining face and behind the open-off cut. Under the influence of tensile and shear stresses the fissures develop gradually. When the medium filled in the expanded fracture is air, the conductivity of the structural plane becomes worse. When the filling medium is water, the conductivity of the structural plane will increase. In addition, vertical tensile fractures and transverse shear fractures are formed in the weathered rock due to the influence of tensile and shear stress, and these fractures expand-develop and interconnect to form a fissure network, and the range of plastic zone is constantly expanding. Simulation results of the stress and plastic zone at 70,

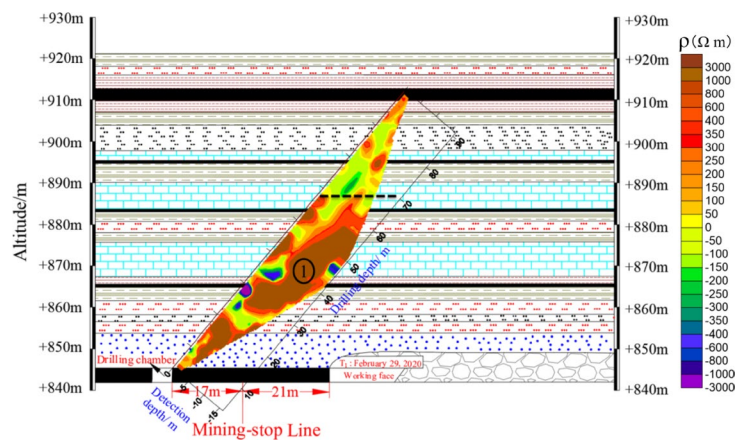
120, 140 and 160 m of working face advance were selected for study. The results show that the failure mode of plastic zone is mainly tensile shear failure mode. The rock mass is destroyed by tensile stress which exceeds its own tensile strength. In addition, the influence of shear stress on the fracture development of rock mass is complex, which is mainly manifested as that after the shear stress acting on the shear plane exceeds the peak shear strength of rock mass, the shear stress will decrease with the increase of rock mass deformation, and the rock mass will be shear-damaged. Under the action of small shear stress, the rock mass will slide along the shear fracture, making the fracture volume increase.

When the working face is advanced 70 m, the maximum development height of the plastic zone is 28 m which is consistent with the distribution height of the maximum shear stress, and the development pattern of the plastic zone is consistent with the distribution pattern of the tensile stress (Fig. 14a). When the working face advanced to 120 m, the development height of the plastic zone was 41.9 m, and the plastic zone gradually changed from arch-shaped

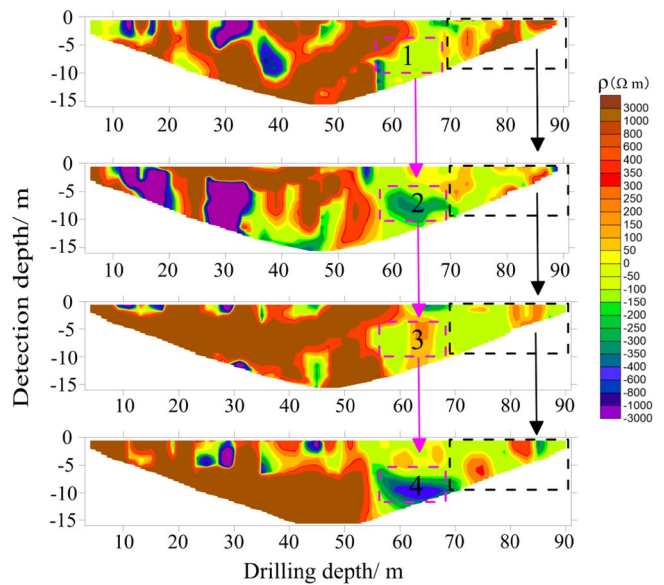
Fig. 13 The overburden failure resistivity profiles in different detection periods



(a) The overburden failure resistivity profiles when the mining face is mined 31 m away from the mining stop line

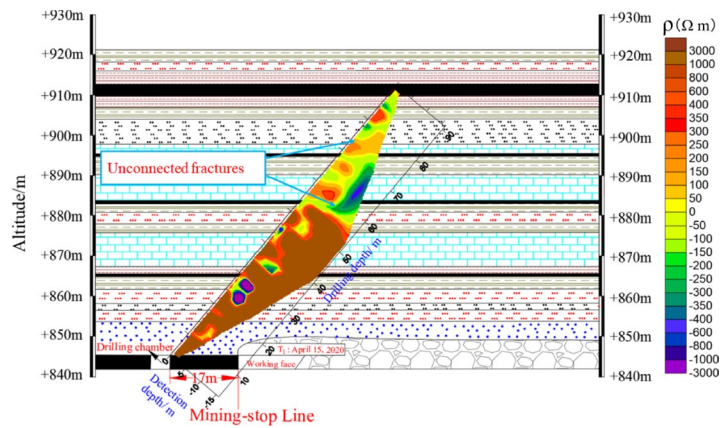


(b) The overburden failure resistivity profiles when the mining face is mined 21 m away from the mining stop line

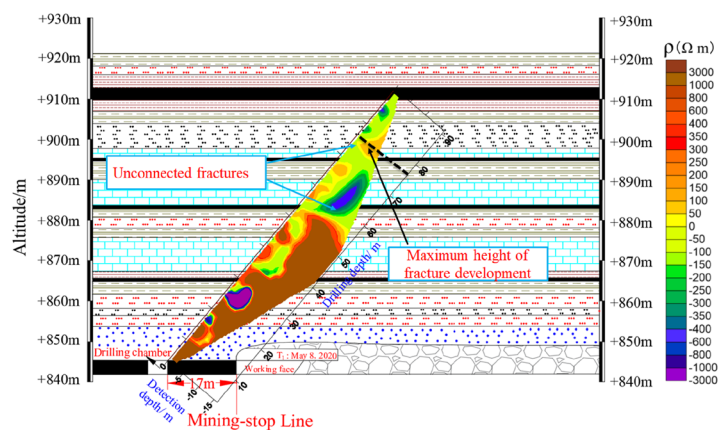


(c) The inversion diagram of apparent resistivity when the coal face advances to 11, 7, 4 and 0 m from the stop line

Fig. 13 (continued)



(d) The overburden failure resistivity profiles after stopping mining for 25 days



(e) The overburden failure resistivity profiles after stopping mining for 40 days

to saddle-shaped, which was due to the influence of larger shear stresses behind the open-off cut and in front of the coal mining face (Fig. 14b). When the working face advanced to 140 m, the plastic zone development height reached the maximum 49.7 m (Fig. 14c), after that, the longitudinal development height of the plastic zone did not change, only the lateral development range increased (Fig. 14d), indicating that the overburden fissure development entered a stable stage. Therefore, the maximum DHOF of No. 9 coal mining was 49.7 m.

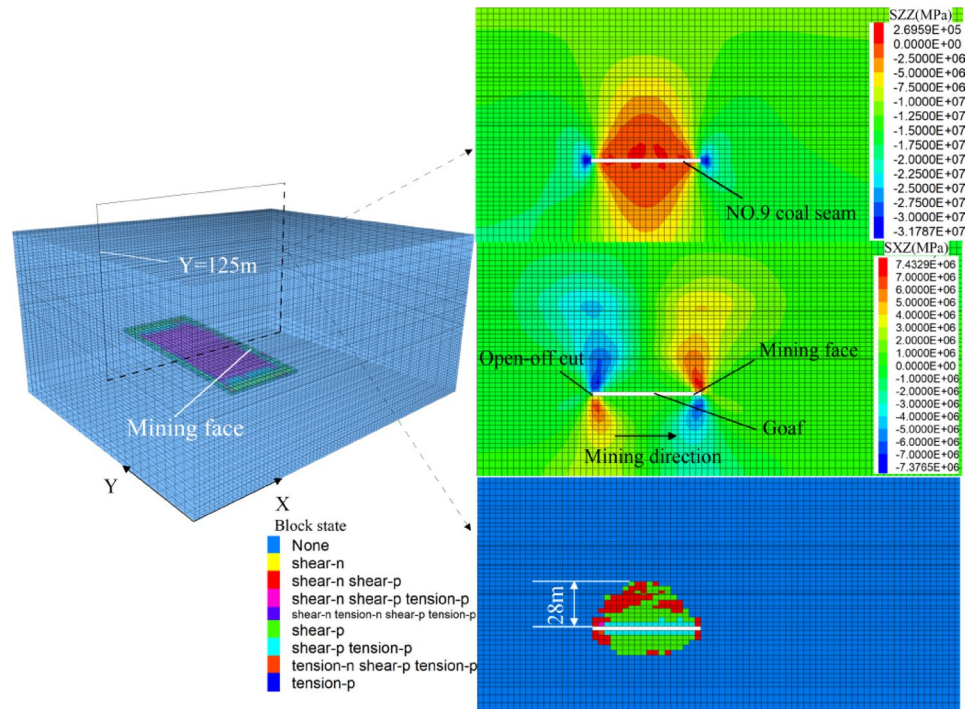
After the No.9 coal was mined and then the upper No. 5 coal was mined, the plastic zone cloud diagram is shown in Fig. 15. The positions of the key strata are consistent with that in Fig. 8. The key strata 1 is coarse sandstone, the key strata 2 and the key strata 3 are limestone, and the key strata 4 is medium sandstone. When the No. 5 coal seam was mined to 90 m, the rock seam near the floor of the open-off cut was damaged by tensile and shear stresses, forming a ‘trapezoidal’ plastic zone where there was a potential risk of water and gas conduction (Fig. 15a). When the No. 5 coal

was mined to 160 m, under the influence of mining stresses, the key strata 4 still maintained good integrity and did not break, and the plastic zone at the base of the No. 5 coal seam was not connected to the plastic zone at the roof of the No. 9 coal (Fig. 15b). Therefore, it was necessary to pre-emptively reinforce the potentially risky areas of the trapezoid prior to mining of the No. 5 coal.

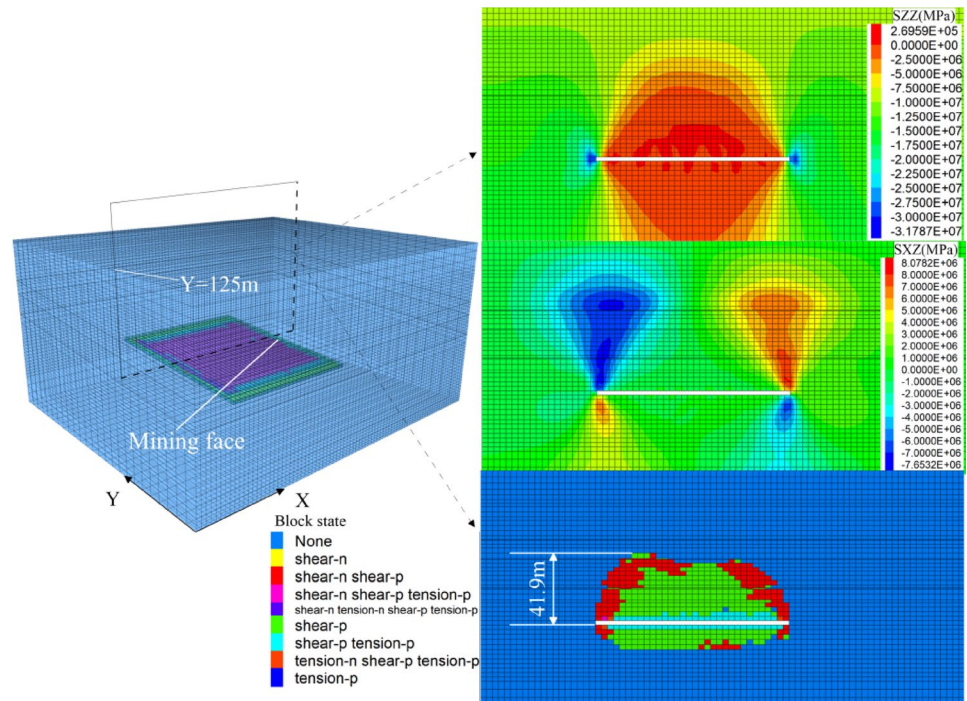
Discussion

In this study, the three research methods of theoretical analysis, field monitoring and numerical simulation were used to obtain the overburden fracture development heights of 52.5 m, 53 m and 49.7 m for the mining of the 9-204 working face of the Dianping Mine, respectively, with a relative error of less than 5% between the three, and, therefore, the results are very reliable. In addition, the results of all three methods show that key strata 4 is not fractured. The

Fig. 14 Simulated 3D perspective view and transverse sectional view of plastic zone and stress distribution

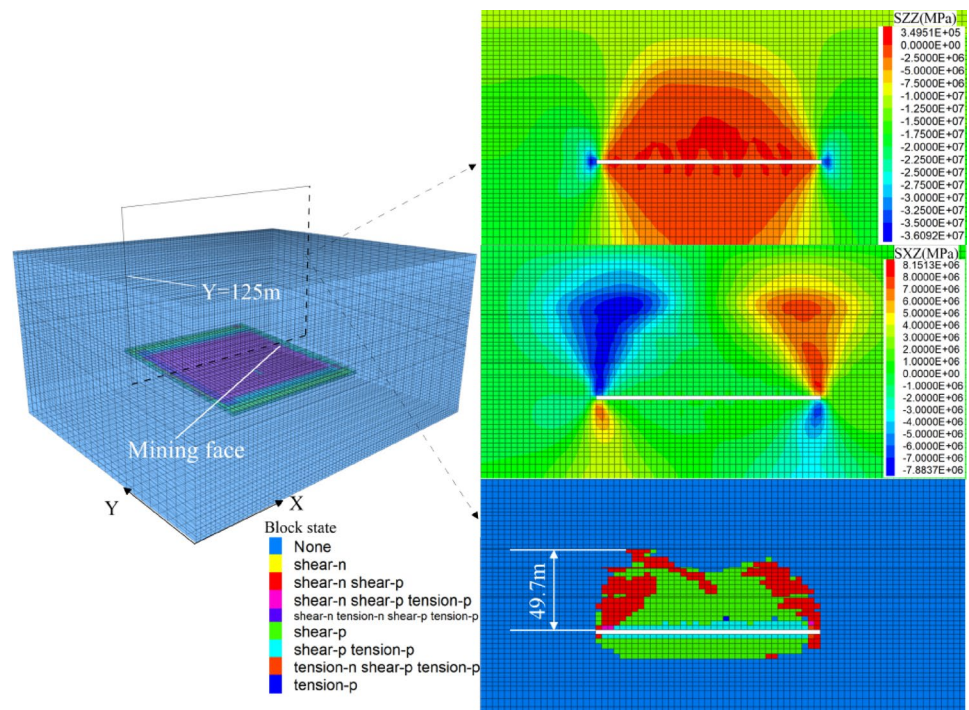


(a) Working face advancing 70 m

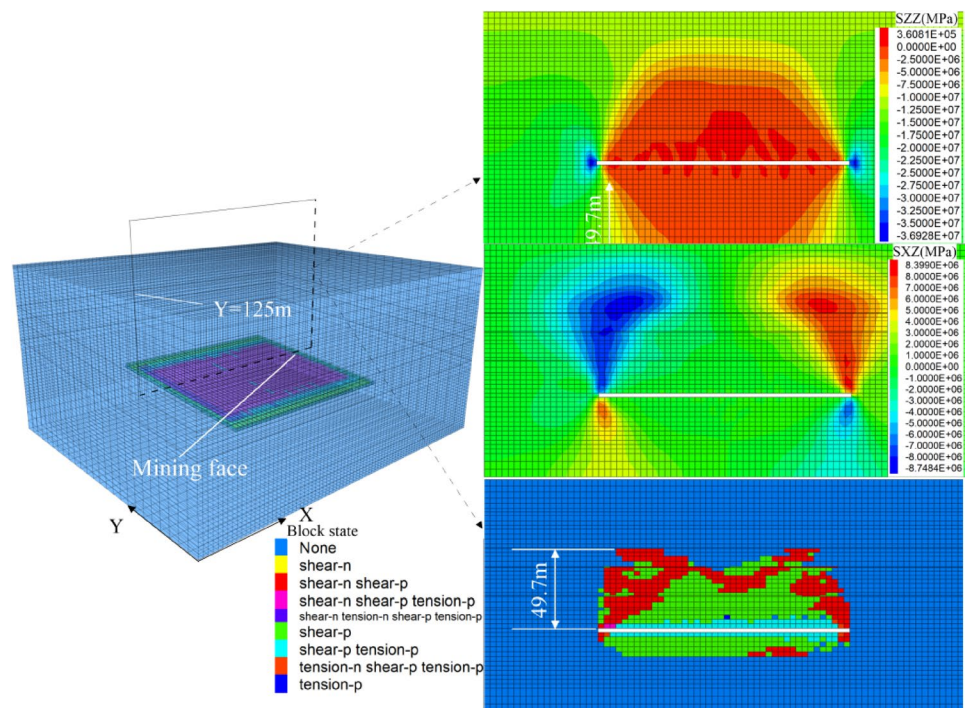


(b) Working face advancing 120 m

Fig. 14 (continued)



(c) Working face advancing 140 m



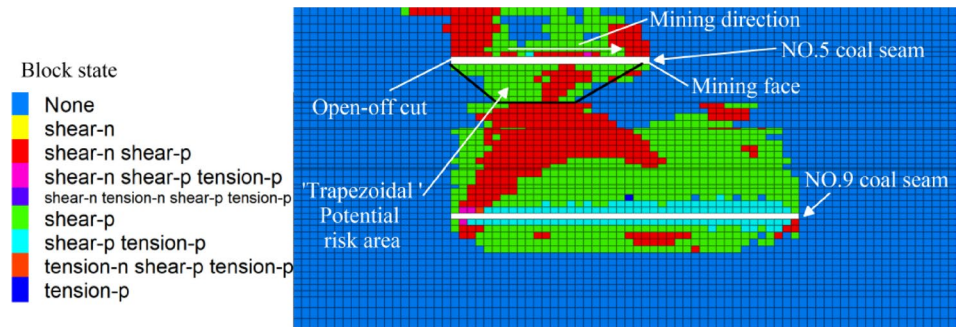
(d) Working face advancing 160 m

numerical simulation results also show that after mining of the upper and lower coal seams are mined, the key strata 4 remains intact and still has good water and gas barrier

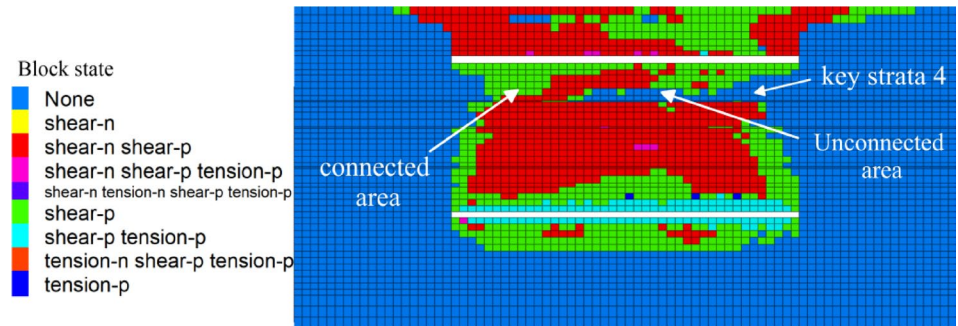
capabilities, so it is entirely feasible to implement upward mining in the Dianping Mine.

The overlying strata of the Taiyuan Formation coal seam in Shanxi, China, are characterized by their

Fig. 15 The numerical profiles of mining-induced failure area



(a) Working face advancing 90 m of NO.5 coal seam



(b) Working face advancing 160 m of NO.5 coal seam

Table 2 Comparison of calculation results

| | Equation (1) | Equation (2) | Height of the fracture development (m) | | Relative error (%) | |
|-----------------------|--|---------------------------------|--|--------------|--------------------|--------------|
| | | | Equation (1) | Equation (2) | Equation (1) | Equation (2) |
| Empirical formula | $H_{li} = \frac{100 \sum M}{1.6 \sum M + 3.6} \pm 5.6$ | $H_{li} = 20\sqrt{\sum M} + 10$ | 39.1 | 42.2 | 26.2 | 20.4 |
| Modified formula | $H_{li} = 4.24 \sum M + 39.8b + 12.8$ | $H_{li} = 12.88 \sum M + 35.42$ | 49.7 | 68.9 | 6.2 | 30.0 |
| Methods in this paper | | | 52.5 | | 0.9 | |
| In situ observation | | | 53.0 | | | |

numerous layers, small thickness, and complex structure. Thus, the fracture development characteristics of overlying strata are different from those of traditional strata. The traditional and the modified correction formulas for calculating the DHOF are compared with the calculation results presented in this paper (He et al. 2020; Wang et al. 2018), as shown in Table 2, In the table, where *b* is the proportion coefficient of hard rock, which is 0.6. The error of the calculation results of the traditional calculation and correction formulas is substantially larger than that of the calculation method proposed in this paper. In addition, Liu et al. proposed to use different calculation methods for hard and soft rocks to calculate rock failure layer-by-layer from bottom to top (Liu et al. 2018). The calculation

process of this method is complicated, and the failure of rock strata is usually not the failure of layer-by-layer rule from bottom to top, thus yielding certain errors. By contrast, the calculation method proposed in this paper first computes the damage of key strata and then analyzes this damage in multiple soft strata controlled by key strata. This method is not only simple in the calculation process but also highly accurate after field measurement verification. The disadvantage is that this method is only applicable to the hard and medium-hard roof conditions, and the weak roof is inapplicable because the hinged structure cannot be formed when the rock stratum is broken.

Conclusions

Taking the 9-204 working face of the Dianping coal mine in Shanxi Province as the research object, theoretical analysis, field measurement, and numerical simulation were used to investigate the fracture development rules of overlying strata and the feasibility of UM. The following conclusions are drawn from this paper.

- (1) Combined with plastic hinge and fixed beam theories, a new calculation method for the height of overburden fracture development is proposed in this paper by analyzing the fracture characteristics of rock strata with different lithologies, and the concept of KSRS is presented. The DHOF after coal mining in No. 9 coal seam is 52.5 m, which is close to the results of field measurement and numerical simulation.
- (2) Based on theoretical analysis, field measurements and numerical simulations, the DHOF at Dianping Mine are 52.5, 53 and 49.7 m. The distance between NO.9 coal seam and No. 5 coal seam is 65 m, so No. 5 coal seam is located in the continuous deformation zone and is less affected by mining. Numerical simulation results show that after the upper and lower coal seams have been mined, the strata between the two coal seams is only connected by a small area of fractures in the vicinity of the open-off cut. Therefore, UM is fully feasible after simple pre-reinforcement treatment of the fracture connection area.
- (3) The dynamic monitoring results of DHOF by the BRM indicate that the fractures in the fractured zones are not completely connected, but that there is a certain range of unconnected fracture areas in the upper part of the fractured zones, where the fractures exist independently of each other. However, the areas are subject to continuous change due to mining stresses and are, therefore, a potential risk.
- (4) The research results provide a theoretical and technical basis for the prediction of overburden fracture development height and the feasibility prediction of UM in the Taiyuan Formation coal field of Shanxi Province.

Acknowledgements This study was supported by The Fundamental Research Funds for the Central Universities (No. 2021YJSDC21).

Funding The Fundamental Research Funds for the Central Universities, 2021YJSDC21.

Declarations

Conflict of interest The authors declare no competing interests.

References

- Adhikary DP, Guo H (2015) Modelling of longwall mining-induced strata permeability change. *Rock Mech Rock Eng* 48(1):345–359. <https://doi.org/10.1007/s00603-014-0551-7>
- Bai JW, Feng GR, Wang SY, Qi TY, Yang J, Guo J, Li Z, Du XJ, Wang ZH, Du YL, Zhang YJ (2018) Vertical stress and stability of interburden over an abandoned pillar working before upward mining: a case study. *Roy Soc Open Sci* 5(8):180346. <https://doi.org/10.1098/rsos.180346>
- Cheng GW, Ma TH, Tang CA, Liu HY, Wang SJ (2017) A zoning model for coal mining - induced strata movement based on microseismic monitoring. *Int J Rock Mech Min Sci* 94:123–138. <https://doi.org/10.1016/j.ijrmms.2017.03.001>
- Cheng GW, Yang TH, Liu HY, Wei LK, Zhao Y, Liu YL, Qian JW (2020) Characteristics of stratum movement induced by downward longwall mining activities in middle-distance multi-seam. *Int J Rock Mech Min Sci* 136:104517. <https://doi.org/10.1016/j.ijrmms.2020.104517>
- Cui F, Jia C, Lai XP (2019a) Study on deformation and energy release characteristics of overlying strata under different mining sequence in close coal seam group based on similar material simulation. *Energies* 12(23):4485. <https://doi.org/10.3390/en12234485>
- Cui F, Yang YB, Lai XP, Cao JT (2019b) Similar material simulation experimental study on rockbursts induced by key stratum breaking based on microseismic monitoring. *Chin J Rock Mech Eng* 38:803–814. <https://doi.org/10.13722/j.cnki.jrme.2018.1423>
- Guo WB, Lou GZ (2018) Definition and distinguishing method of critical mining degree of overburden failure. *J China Coal Soc* 44(3):755–766. <https://doi.org/10.13225/j.cnki.jccs.2018.6038>
- He X, Zhao YX, Zhang C, Han PH (2020) A model to estimate the height of the water-conducting fracture zone for longwall panels in Western China. *Mine Water Environ* 39(4):1–16. <https://doi.org/10.1007/s10230-020-00726-2>
- Hou GY, Hu T, Li ZX, Xie BB, Zhou XHL, TC, (2020) Fiber optic strain characterization of “two zones” deformation of overburden mining based on BOFDA. *J Min Saf Eng* 37:224–237. <https://doi.org/10.13545/j.cnki.jmse.2020.02.002>
- Hu T, Hou G, Bu S, Zhu Z, Wang Y, Hu ZY, Li ZX (2020a) A novel approach for predicting the height of water-conducting fracture zone under the high overburden caving strength based on optimized processes. *Processes* 8(8):950. <https://doi.org/10.3390/pr8080950>
- Hu T, Hou G, Li Z (2020b) The field monitoring experiment of the roof strata movement in coal mining based on DFOS. *Sensors* 20(5):1318. <https://doi.org/10.3390/s20051318>
- Huang BX, Liu CY, Xu JL (2010) Research on through degree of overlying strata fracture fissure induced by mining. *J China U Min Techno* 39(1):45–49
- Huang WP, Li C, Zhang LW, Yuan Q, Zheng YS, Liu Y (2018) In situ identification of water-permeable fractured zone in overlying composite stratum. *Int J Rock Mech Min Sci* 105:85–97. <https://doi.org/10.1016/j.ijrmms.2018.03.013>
- Karacan C, Goodman G (2009) Hydraulic conductivity changes and influencing factors in longwall overburden determined by slug tests in gob gas ventholes. *Int J Rock Mech Min Sci* 46(7):1162–1174. <https://doi.org/10.1016/j.ijrmms.2009.02.005>
- Li Z, Xu Y, Li L, Zhai C (2015) Forecast of the height of water flowing fractured zone based on BP neural networks. *J Min Safety Eng* 32:905–910. <https://doi.org/10.13545/j.cnki.jmse.2015.06.006>
- Liang Z, Song W, Liu W (2020) Theoretical models for simulating the failure range and stability of inclined floor strata induced by mining and hydraulic pressure. *Int J Rock Mech Min Sci* 132:104382. <https://doi.org/10.1016/j.ijrmms.2020.104382>

- Liu SL, Li WP, Wang QQ, Pei YB (2018) Investigation on mining-induced fractured zone height developed in different layers above Jurassic coal seam in western China. *Arab J Geosci* 11(2):30. <https://doi.org/10.1007/s12517-018-3383-z>
- Liu X, Tan Y, Ning J, Tian C, Wang J (2015) The height of water-conducting fractured zones in longwall mining of shallow coal seams. *Geotech Geol Eng* 33:693–700. <https://doi.org/10.1007/s10706-015-9851-2>
- Liu Y, Liu QM, Li WP, Li T, He JH (2019) Height of water-conducting fractured zone in coal mining in the soil–rock composite structure overburdens. *Environ Earth Sci* 78(7):242. <https://doi.org/10.1007/s12665-019-8239-7>
- Majidi A, Hassani F, Nasiri M (2012) Prediction of the height of distressed zone above the mined panel roof in longwall coal mining. *Int J Coal Geol* 98:62–72. <https://doi.org/10.1016/j.coal.2012.04.005>
- Qian MG, Shi PW, Xu JL (2010) *Mine pressure and strata control*. China University of Mining and Technology Press, Xuzhou
- Ren Z, Wang N (2020) The overburden strata caving characteristics and height determination of water conducting fracture zone in fully mechanized caving mining of extra thick coal seam. *Geotech Geol Eng* 38(1):329–341. <https://doi.org/10.1007/s10706-019-01019-4>
- Sun Y, Zuo J, Karakus M, Wang J (2019) Investigation of movement and damage of integral overburden during shallow seam mining. *Int J Rock Mech Min Sci* 117:63–75. <https://doi.org/10.1016/j.ijrmms.2019.03.019>
- Sun YJ, Zuo JP, Murat K, Jinhao W (2020) A novel method for predicting movement and damage of overburden caused by shallow coal mining. *Rock Mech Rock Eng* 53(4):1545–1563. <https://doi.org/10.1007/s00603-019-01988-1>
- Wang F, Xu J, Chen S, Ren MZ (2019) Method to predict the height of the water conducting fractured zone based on bearing structures in the overlying strata. *Mine Water Environ* 38(4):767–779. <https://doi.org/10.1007/s10230-019-00638-w>
- Wang YG, Guo WB, Bai EH, Zhang ZY, Kang YP, Chai HB, Chen JJ (2018) Characteristics and mechanism of overlying strata movement due to high-intensity mining. *J China Coal Soc* 43(S1):28–35. <https://doi.org/10.13225/j.cnki.jccs.2017.1423>
- Wei JC, Wu FZ, Yin HY, Guo JB, Xie DL, Xiao LL, Zhi HF, Leticariu L (2017) Formation and height of the interconnected fractures zone after extraction of thick coal seams with weak overburden in Western China. *Mine Water Environ* 36(1):59–66. <https://doi.org/10.1007/s10230-016-0396-2>
- Wu BY, Deng ZG, Feng YF (2017a) Li F (2017a) analysis of the influence of interlayer rock on ascending mining under special conditions. *J China Coal Soc* 42(4):842–848. <https://doi.org/10.13225/j.cnki.jccs.2016.0621>
- Wu YP, Gao XC (2010) Experimental comparative study on lateral deformation characteristics of coal sample in different loading path. *J China Coal Soc* 35(S0):44–48. <https://doi.org/10.13225/j.cnki.jccs.2010.s1.015>
- Wu Q, Shen J, Liu W, Wang Y (2017b) A RBFNN-based method for the prediction of the developed height of a water-conductive fractured zone for fully mechanized mining with sublevel caving. *Arab J Geosci* 10(7):172. <https://doi.org/10.1007/s12517-017-2959-3>
- Yang XB, Han XX, Liu EL, Zhang ZP, Wang TJ, Zhang LH (2018) Properties of non-uniform deformation evolution of rock under uniaxial cyclic loading and unloading. *J China Coal Soc* 43(2):449–456. <https://doi.org/10.13225/j.cnki.jccs.2017.1119>
- Zhang KG (2016) *Bearing Capacity of Spreading Foundation on Finite Element and Plastic Hinge Theory Analysis*. Dissertation, Chongqing University
- Zhang TJ, Zhang L, Li SG, Zhang C, Song S, Bao RY (2017) Characteristics of the surface deformation of specimens with a hole during the progressive failure. *J China Coal Soc* 42(10):2623–2630. <https://doi.org/10.13225/j.cnki.jccs.2017.0022>
- Zhang Y, Cao SG, Gao R, Guo S, Lan LX (2018) Prediction of the heights of the water-conducting fracture zone in the overlying strata of short wall block mining beneath aquifers in western China. *Sustainability* 10(5):1636. <https://doi.org/10.3390/su10051636>
- Zhao CH, Jin DW, Wang H, Wang QM, Wang SD, Liu Y (2019a) Construction and application of overburden damage and aquifer water loss model in medium-deep buried coal seam mining in Yushen mining area. *J China Coal Soc* 44(7):2227–2235. <https://doi.org/10.13225/j.cnki.jccs.2019.0159>
- Zhao ZL, Jing HW, Shi XS, Han GS (2019b) Experimental and numerical study on mechanical and fracture behavior of rock-like specimens containing pre-existing holes flaws. *Eur J Environ Civ En*. <https://doi.org/10.1080/19648189.2019.1657961>
- Zhong CM (2011) *Research on movement and deformation rules of rock strata between coal seams in caving method up ward mining of left-over coal with numerical simulation*. Dissertation, Taiyuan University of Technology
- Zhu T, Li W, Wang Q, Fan K, Du J (2020) Study on the height of the mining-induced water-conducting fracture zone under the Q₂₁ loess cover of the Jurassic coal seam in northern Shaanxi, China. *Mine Water Environ* 39(1):57–67. <https://doi.org/10.1007/s10230-020-00656-z>
- Zhou Z (2017) *Study on the development law of mining fracture and karst surface collapse when mining in karst area*. Dissertation, Hunan University of Science And Technology

Publisher's Note Springer Nature remains neutral with regard to jurisdictional claims in published maps and institutional affiliations.

Springer Nature or its licensor holds exclusive rights to this article under a publishing agreement with the author(s) or other rightsholder(s); author self-archiving of the accepted manuscript version of this article is solely governed by the terms of such publishing agreement and applicable law.